Dual Quaternion Based Finite-Time Tracking Control for Mechatronic Systems with Actuation Allocation

Lichao Sun
School of Education, Communication & Society
King's College London
London, United Kingdom
lichao.sun@kcl.ac.uk

Yanpei Huang
Department of Bioengineering
Imperial College London
London, United Kingdom
yanpei.huang@imperial.ac.uk

Ziwei Wang
Department of Bioengineering
Imperial College London
London, United Kingdom
ziwei.wang@ieee.org

Bo Xiao
Department of Computing
Imperial College London
London, United Kingdom
b.xiao@imperial.ac.uk

Eric M. Yeatman
Department of Electrical and Electronic Engineering
Imperial College London
London, United Kingdom
e.yeatman@imperial.ac.uk

***Abstract*—This paper investigates the tracking control performance regulation and actuation allocation of mechatronic systems subject to coupling motions. In particular, the kinematic and dynamic model is described by dual quaternion, which captures the coupling effect between translation and rotation movements. Considering external disturbances and system uncertainties, a non-singular fast terminal sliding controller is then developed to ensure finite-time tracking performance. In addition, the unwinding problem caused by the redundancy of dual quaternion is addressed with the help of a novel attitude error function. Furthermore, an improved simplex method is designed for distributing the developed control commands to proper actuators. Numerical simulations demonstrate the effectiveness with respect to disturbance suppression, fast tracking, high accuracy, and finite-time stability of the proposed method.**

***Index Terms*—Dual quaternion, sliding mode control, finite-time stability, control allocation.**

I. Introduction

High-Performance control of mechanical systems has attracted concerns from the fields of space [1], [2], surgery [3], [4], and human-robot interaction [5], [6]. However, proximate interaction tasks can be featured by coupling effect between translation and orientation motions. As a result, unified control design that addresses such coupling issue is still challenging. By developing a velocity-free nonlinear controller based on dual quaternion, the relative position and attitude of a rigid body were globally asymptotic stable [7]. The subsequent works based on dual quaternion become promising, but lack the consideration of control performance. For faster convergence performance, the finite-time controller was realized via terminal sliding mode [8], [9]. However, the above control implementation might suffer from singularity. Recently, increasing plants are equipped with redundant sets of actuators. With respect to over-actuated systems, control allocation aims to distribute the desired control command among the redundant actuators. To achieve the optimum with certain constraints, the fixed, single-gimbal, and double-gimbal thruster configurations were considered in [10]. In [11], a power-optimal reaction wheel motor torque distribution strategy was developed to minimize the instantaneous electrical power requirement.

In this paper, a non-singular fast terminal sliding mode (NFTSM) control strategy is developed to ensure finite-time convergence of state errors. In addition, the unwinding problem caused by the redundancy of dual quaternion is addressed through a novel attitude error function. Furthermore, optimization algorithm is adopted in control allocation to alleviate the physical restrictions on actuation characteristics and limitation of the maximal force based on null space. The main contributions of this paper are twofold: 1) The coupling phenomenon between translation and orientation motions is systematically addressed by dual quaternion while ensuring finite-time and unwinding-free convergence. 2) Control allocation is modelled as an optimal quadratic programming, which extends the application of traditional pseudo-inverse method.

This work was supported in part by the U.K. EPSRC under Grant EP/P012779/1.

II. Preliminaries

A. Dual Quaternion

In order to tackle 6-degree-of-freedom (DoF) tracking issue, we introduce dual quaternion $\hat{q}$ to describe the translational and rotational motion simultaneously [12]: $\hat{q} := q + \epsilon q'$, where q and q' denote the real and dual part, respectively. ϵ is the dual operator such that $\epsilon^2 = 0$, $\epsilon \neq 0$. Regarding $\hat{a} = a + \epsilon a'$

and $\hat{b} = b + \epsilon b'$, the following properties are presented for later derivation:

$$\hat{a} \pm \hat{b} := a \pm b + \epsilon(a' \pm b'), \quad \hat{a}^* := a + \epsilon(-a'), \tag{1}$$

$$\hat{a} \times \hat{b} := a \times b + \epsilon(a \times b' + a' \times b), \hat{a} \odot \hat{b} := ab + \epsilon a' b', \tag{2}$$

$$< \hat{a}, \hat{b} > := ab + a'b', \qquad [\hat{a}|\hat{b}] := a^{\mathrm{T}} b' + a'^{\mathrm{T}} b, \tag{3}$$

$$\hat{a} \circ \hat{b} := ab - a'b' + \epsilon(ab' + a'b + a' \times b'), \tag{4}$$

$$\hat{a} \leq \hat{b} \quad \text{i.f.f.} \quad a \leq b \,\text{AND}\, a' \leq b'. \tag{5}$$

With the definition of desired pose $\hat{q}_d$, the dual quaternion error can be written as:

$$\hat{q}_e = \hat{q}_d^* \circ \hat{q} = q_e + \epsilon \frac{1}{2} q_e \circ p_e \tag{6}$$

where q_e and p_e are the quaternion and position error, respectively. Calculating the derivative of $\hat{q}_e$ yields the relative kinematics based on dual quaternion error:

$$\dot{\hat{q}}_e = \frac{1}{2} \hat{q}_e \circ \hat{\omega}_e, \hat{\omega}_e := \hat{\omega} - \hat{q}_e^* \circ \hat{\omega}_d \circ \hat{q}_e, \tag{7}$$

in which $\hat{\omega}$ and $\hat{\omega}_d$ are the actual and desired velocity motor. Therefore, taking the time derivative of $\dot{\hat{q}}_e$ follows

$$\hat{M}\dot{\hat{\omega}}_e = \hat{u} + \hat{M}[\hat{\omega}_e \times (\hat{q}_e^* \circ \hat{\omega}_d \circ \hat{q}_e) - \hat{q}_e^* \circ \dot{\hat{\omega}}_d \circ \hat{q}_e] - \hat{\omega} \times \hat{M}\hat{\omega} \tag{8}$$

where $\hat{M} = m \frac{d}{d} I + \epsilon J$ is the dual inertial matrix, m the mass, J the inertia matrix, I the identity matrix with appropriate dimension. $\hat{u}$ is dual force vector such that

$$\hat{u} = \hat{u}_c + \hat{u}_d = u_c + u_d + \epsilon(\tau_c + \tau_d), \tag{9}$$

where u_c and τ_c are the control force and torque. u_d and τ_d are the external force and torque disturbance.

III. Control Law Design

Considering the dexterous 6-DoF trajectory tracking task, the control objective can be stated as: for a class of mechatronic systems (8), design a dual controller $\hat{u}_c = u_c + \epsilon \tau_c$ to make relative error state variables converge in finite time under all time and physically realizable initial conditions. That is, $\hat{\xi}_e := (q_e)_v + \epsilon (q_e')_v \to [0,0,0]^{\mathrm{T}} + \epsilon [0,0,0]^{\mathrm{T}}$ and $\hat{\omega}_e \to \hat{0}$, where $(\cdot)_v$ denotes the vector part of quaternion. For ease of the controller design and analysis, the following lemma is required.

Lemma1 [13]. It is assumed that there exists a continuously differentiable function $V : U \to \mathbb{R}$, which satisfies the following conditions: (1) V is a positive-definite function; (2) There exist positive constants γ, $\alpha \in (0,1)$, and an open neighborhood including $U_0 \subset U$, in which $\dot{V}(x) + \gamma V \ (x)$is negative semi-definite (x is the system state). Then the equilibrium of system trajectory is finite-time stable. Moreover, if $U_0 = U = \mathbb{R}$, the system is globally finite-time stable and the settling time T satisfies $T \leq \frac{V_0^{1-}}{(1- \ )}$, in which V_0 is the initial value of V.

Considering the external disturbances and system uncertainties, kinematics and dynamics are equivalent to:

$$\begin{aligned} \dot{\hat{\xi}}_e &= \hat{\Theta}(\hat{q}_e)\hat{\omega}_e, \\ \hat{M}_0 \dot{\hat{\omega}}_e &= \hat{u}_c + \hat{M}_0[\hat{\omega}_e \times (\hat{q}_e^* \circ \hat{\omega}_d \circ \hat{q}_e) - \hat{q}_e^* \circ \dot{\hat{\omega}}_d \circ \hat{q}_e] \\ &\quad - \hat{\omega} \times \hat{M}_0 \hat{\omega} + \hat{\Phi}, \end{aligned} \tag{10}$$

where $\hat{\Theta}(\hat{q}_e) = \frac{1}{2}(\hat{\eta}_e I + \hat{\xi}_e^{\times})$ with $\dot{\hat{\eta}}_e = -0.5 \hat{\eta}_e^{\mathrm{T}} \hat{\omega}_e$. $(\cdot)^{\times}$ is the cross product matrix operator. $\hat{M}_0$ and $\Delta\hat{M}$ the nominal and uncertain part of $\hat{M}$ such that $\hat{M} = \hat{M}_0 + \Delta\hat{M}$ and therefore $\hat{\Phi}$ can be written as:

$$\begin{aligned} \hat{\Phi} = -\Delta\hat{M}\dot{\hat{\omega}}_e + \Delta\hat{M}[\hat{\omega}_e \times (\hat{q}_e^* \circ \hat{\omega}_d \circ \hat{q}_e) - \hat{q}_e^* \circ \dot{\hat{\omega}}_d \circ \hat{q}_e] \\ - \hat{\omega} \times \Delta\hat{M}\hat{\omega} + \hat{u}_d. \end{aligned} \tag{11}$$

To realize the control objective, the terminal sliding mode (TSM) [14] is modified as dual form:

$$\hat{S}_i = S_i + \epsilon S_i' = \dot{\hat{\xi}}_{ei} + \hat{b}_i \odot \text{sig}(\hat{\xi}_{ei}) \ \ , i = 1,2,3, \tag{12}$$

where $\hat{S} = [\hat{S}_1, \hat{S}_2, \hat{S}_3]^{\mathrm{T}}$, $\text{sig}(\hat{\xi}_{ei}) \ = \text{sig}(\xi_{ei}) \ + \epsilon \text{sig}(\xi_{ei}') \ $, $\text{sig}(\cdot) = \text{sgn}(\cdot)|\cdot| \ $. $\text{sgn}(\cdot)$ is the sign function. $\alpha \in (0,1)$. $\hat{b}_i = b_i + \epsilon b_i'$ with b_i and b_i' being positive constants. Based on terminal sliding surface (12), the conventional TSM controller can be then designed as the similar structure in [15]. Unfortunately, the above algorithm implementation might not be well posed since the negative index term containing may cause singularity. In consideration of physical input saturation of the practical actuators, the aforementioned controller outputs tend to result in instability of the closed-loop system.

Inspired by [16], a variant of the non-singular fast terminal sliding mode (NFTSM) in dual form is proposed to eliminate the singularity phenomenon and improve the convergence rate

$$\hat{S}_i = \dot{\hat{\xi}}_{ei} + \hat{\alpha}_{1i} \odot \hat{\xi}_{ei} + \hat{\alpha}_{2i} \odot \hat{S}_{ai}, i = 1,2,3, \tag{13}$$

where $\hat{\alpha}_{1i} = \alpha_{1i} + \epsilon \alpha_{1i}'$, $\hat{\alpha}_{2i} = \alpha_{2i} + \epsilon \alpha_{2i}'$. α_{1i}, α_{1i}', α_{2i}, and α_{2i}' are positive constants. The auxiliary terminal sliding surface is designed as:

$$S_{ai} = \begin{cases} \text{sig}(\xi_{ei})^{p_1}, \text{if } \bar{S}_i = 0 \text{ or } \bar{S}_i \neq 0, |\xi_{ei}| \geq \delta \\ r_1 \xi_{ei} + r_2 \text{sig}(\xi_{ei})^2, \text{if } \bar{S}_i \neq 0, |\xi_{ei}| < \delta \end{cases} \tag{14}$$

$$S_{ai}' = \begin{cases} \text{sig}(\xi_{ei}')^{p_1}, \text{if } \bar{S}_i' = 0 \text{ or } \bar{S}_i' \neq 0, |\xi_{ei}'| \geq \delta' \\ r_1' \xi_{ei}' + r_2' \text{sig}(\xi_{ei}')^2, \text{if } \bar{S}_i' \neq 0, |\xi_{ei}'| < \delta' \end{cases} \tag{15}$$

$$\hat{\bar{S}}_i = \bar{S}_i + \epsilon \bar{S}_i' = \dot{\hat{\xi}}_{ei} + \hat{\alpha}_{1i} \odot \hat{\xi}_{ei} + \hat{\alpha}_{2i} \odot \text{sig}(\hat{\xi}_{ei})^{p_1} \tag{16}$$

where $r_1 = (2 - p_1)\delta^{p_1 - 1}$, $r_1' = (2 - p_1)\delta'^{p_1 - 1}$, $r_2 = (p_1 - 1)\delta^{p_1 - 2}$, and $r_2' = (2 - p_1)\delta'^{p_1 - 2}$. δ and δ' are small positive constants. $p_1 \in (0.5, 1)$ is a positive constant. To achieve the control objective, an NFTSM based control law is proposed as:

$$\begin{aligned} \hat{u}_c = &- \hat{M}_0[\hat{\omega}_e \times (\hat{q}_e^* \circ \hat{\omega}_d \circ \hat{q}_e) - \hat{q}_e^* \circ \dot{\hat{\omega}}_d \circ \hat{q}_e] + \hat{\omega} \times \hat{M}_0 \hat{\omega} \\ &- \hat{K}\text{sgn}(\hat{S}) - (\hat{M}_0 \hat{\Theta}(\hat{q}_e)^{-1})[\hat{\alpha}_1 \odot \dot{\hat{\xi}}_e + \dot{\hat{\Theta}}(\hat{q}_e)\hat{\omega}_e \\ &+ \hat{\alpha}_2 \odot W(\hat{\xi}_e) \odot \hat{\Theta}(\hat{q}_e)\hat{\omega}_e + \hat{\alpha}_3 \odot \text{sig}(\hat{S})^{p_2}] \end{aligned} \tag{17}$$

where $\hat{\alpha}_3 = \alpha_3 + \epsilon\alpha_3'$ and $\hat{K} = K + \epsilon K'$. α_3, α_3', K, K', and p_2 are positive constants. Diagonal matrix $W(\hat{\xi}_e)$ is the auxiliary switching term, whose i-th entry is designed as:

$$W(\xi_{ei}) = \begin{cases} p_1 |\xi_{ei}|^{p_1-1}, \text{if } \bar{S}_i = 0 \text{ or } \bar{S}_i \neq 0, |\xi_{ei}| \geq \delta \\ r_1 + 2r_2 |\xi_{ei}|, \text{if } \bar{S}_i \neq 0, |\xi_{ei}| < \delta \end{cases} \tag{18}$$

$$W(\xi_{ei}') = \begin{cases} p_1 |\xi_{ei}'|^{p_1-1}, \text{if } \bar{S}_i' = 0 \text{ or } \bar{S}_i' \neq 0, |\xi_{ei}'| \geq \delta' \\ r_1' + 2r_2' |\xi_{ei}'|, \text{if } \bar{S}_i' \neq 0, |\xi_{ei}'| < \delta' \end{cases} \tag{19}$$

Theorem 1: Consider dual quaternion based system (8) with external disturbances and system uncertainties that satisfy the bounded assumptions, within control law (17), then the relative dual quaternion and relative velocity motor are guaranteed to converge in finite time.

Proof. Consider the following Lyapunov function candidate: $V_1 = \frac{1}{2}[\hat{S}|\hat{M}_0\hat{S}]$. Taking the time-derivative of V_1 and substituting (10) into it yield

$$\begin{aligned} \dot{V}_1 =& [\hat{S}|\hat{M}_0\ddot{\hat{\xi}}_e + \hat{M}_0\hat{\alpha}_1 \odot \dot{\hat{\xi}}_e + \hat{M}_0\hat{\alpha}_2 \odot \dot{\hat{S}}_a] \\ =& \Big[\hat{S}|\hat{M}_0\dot{\hat{\Theta}}(\hat{q}_e)\hat{\omega}_e + \hat{M}_0\hat{\alpha}_1 \odot \dot{\hat{\xi}}_e + \hat{M}_0\hat{\alpha}_2 \odot \dot{\hat{S}}_a \\ &+ \hat{M}_0\hat{\Theta}(\hat{q}_e)\hat{M}_0^{-1}\big(\hat{u}_c + \hat{M}_0[\hat{\omega}_e \times (\hat{q}_e^* \circ \hat{\omega}_d \circ \hat{q}_e) \\ &- \hat{q}_e^* \circ \dot{\hat{\omega}}_d \circ \hat{q}_e] - \hat{\omega} \times \hat{M}_0\hat{\omega} + \hat{\Phi}\big)\Big]. \end{aligned} \tag{20}$$

Combining the controller (17) with (20) is given by

$$\begin{aligned} \dot{V}_1 \leq & \Big[\hat{S}|\hat{M}_0\hat{\alpha}_2 \odot \dot{\hat{S}}_a - \hat{M}_0\hat{\Theta}(\hat{q}_e)\hat{M}_0^{-1}\hat{K}\text{sgn}(\hat{S}) \\ &- \hat{M}_0\big(\hat{\alpha}_2 \odot W(\hat{\xi}_e)\big) \odot \big(\hat{\Theta}(\hat{q}_e)\hat{\omega}_e + \hat{\alpha}_3 \odot \text{sig}(\hat{S})^{p_2} \\ &+ \hat{M}_0\hat{\Theta}(\hat{q}_e)\hat{M}_0^{-1}\hat{\Phi}\big)\Big] \\ \leq & \Big[\hat{S}| - \hat{M}_0\hat{\alpha}_3 \odot \text{sig}(\hat{S})^{p_2}\Big] \\ \leq & -\underline{\mu}_1\left(\|S_i\|^{p_2} + \|S_i'\|^{p_2}\right) \leq -\mu_1 V_1^{\frac{p_2+1}{2}} \end{aligned} \tag{21}$$

where $\mu_1 = \underline{\mu}_1\sqrt{2/\max\{\sigma_{\max}(J), m\}}$, $\sigma_{\max}(\cdot)$ is the maximum eigenvalue. Thus, based on Lemma 1, the state trajectory of the resulting closed-loop system is guaranteed to reach the sliding mode in finite time. Then, one can obtain

$$\dot{\hat{\xi}}_{ei} = -\hat{\alpha}_{1i} \odot \hat{\xi}_{ei} - \hat{\alpha}_{2i} \odot \hat{S}_{ai}, i = 1, 2, 3. \tag{22}$$

Consider the following Lyapunov function: $V_2 = \frac{1}{2} < \hat{\xi}_e|\hat{\xi}_e >$. Then the derivation of V_2 with respect to time follows

$$\begin{aligned} \dot{V}_2 = -\sum_{i=1}^{3}\Big(& \alpha_{1i}|\xi_{ei}|^2 + \alpha_{1i}'|\xi_{ei}'|^2 + \alpha_{2i}|\xi_{ei}|^{p_1+1} \\ &+ \alpha_{2i}'|\xi_{ei}'|^{p_1+1}\Big) \leq -\mu_2 V_2^{\frac{1+p_1}{2}}. \end{aligned} \tag{23}$$

Accordingly, based on Lemma 1, state variables are guaranteed to converge in finite time, namely $\hat{\xi}_e \to [0, 0, 0]^{\mathrm{T}} + \epsilon[0, 0, 0]^{\mathrm{T}}$ and $\hat{\omega}_e \to \hat{0}$.

Remark 1: The fast terminal sliding mode will switch into asymptotic one when state variables approach zero in (17). It is guaranteed that the state variables will converge within finite settling time during the sliding phase if μ_2 and p_1 are chosen properly. It is further noted that K and K' are control gains, which are suggested to be large enough for the robust stability.

Remark 2: The traditional TSM controller tends to cause singularity because of the negative index term with the state variables converging to zero. Whereas, the proposed control law is non-singular due to the following facts:

1) $\hat{\bar{S}} \neq \hat{0}$. State variables are not small enough to cause singularity. Thus, the control law (17) is obviously non-singular.

2) $\hat{\bar{S}} = \hat{0}$. Then the control law can be re-written as

$$\begin{aligned} \hat{u}_c =& -\hat{M}_0[\hat{\omega}_e \times (\hat{q}_e^* \circ \hat{\omega}_d \circ \hat{q}_e) - \hat{q}_e^* \circ \dot{\hat{\omega}}_d \circ \hat{q}_e] + \hat{\omega} \times \hat{M}_0\hat{\omega} \\ &- \hat{K}\text{sgn}(\hat{S}) - (\hat{M}_0\hat{\Theta}(\hat{q}_e)^{-1})[\hat{\alpha}_1 \odot \dot{\hat{\xi}}_e + \dot{\hat{\Theta}}(\hat{q}_e)\hat{\omega}_e \\ &+ p_1\hat{\alpha}_2 \odot \text{sig}(\hat{\xi}_e)^{2p_1-1} + \hat{\alpha}_3 \odot \text{sig}(\hat{S})^{p_2}]. \end{aligned} \tag{24}$$

Therefore, the singularity will not occur in the case of $p_1 \in (0.5, 1)$.

Remark 3: Double value of quaternions makes the attitude slewing unwinding, which descends the effectiveness and global stability of proposed controller. To eliminate the unwinding problem, two anti-unwinding attitude error functions were presented in [17]. However, discontinuity points exist if $\psi_1 = 2(1 - |q_0|)$ is adopted, and the respond rate declines depends on the attitude error if $\psi_1 = 2(1 - q_0^2)$. For global controller design, a novel attitude error function is proposed in this paper as follows:

$$\phi = 2\left(\lambda_1 + \lambda_2 q_{e0}^2 - \exp\left(\sqrt{\frac{q_{e0}^2}{q_{e0}^2 + \mu}}\right)\right), \tag{25}$$

$$e_r = \left(\exp\left(\sqrt{\frac{q_{e0}^2}{q_{e0}^2 + \mu}}\right)\frac{q_{e0}(|q_{e0}| + 2\mu)}{(|q_{e0}| + \mu)^2}\right)(q_e)_v. \tag{26}$$

where λ_1, λ_2, and μ are positive constants. q_{e0} is the real part of q_e.

Remark 4: The proposed attitude error vector is obviously continuous and bounded with $\theta \in [-\pi, \pi]$, which is shown in Fig. 1. The proposed anti-unwinding method guarantees response rate of the attitude error vector and continuity of the attitude error function simultaneously. Thus, the anti-unwinding NFTSM controller can be easily obtained by replacing the original attitude error function and vector with (25)-(26). It can be further derived that anti-unwinding state variable is updated as $\hat{\xi}_e^* = e_r + \epsilon(e_r \circ p_e)$. Therefore, the sliding mode structure and controller based on new state variable are unwinding-free.

IV. Actuation Allocation

To improve reliability and safety, redundant actuators are often equipped with modern mechanical systems to provide corresponding forces and torques. Inspired by [18], consider the following constraint condition in dual framework

$$\hat{u}_c = \hat{D} \odot \hat{u}_a \tag{27}$$

where $\hat{u}_a$ denotes the control vector applied in redundant actuators, and $\hat{D}$ is control allocation matrix. Note that if there is no uncertainty due to the actuator faults, the pseudo inverse (PI) control allocation can be realized as follows

$$\hat{u}_a = \hat{D}^{\mathrm{T}} \odot (\hat{D} \odot \hat{D}^{\mathrm{T}})^{-1} \odot \hat{u}_c. \tag{28}$$

A. Null Space Based Pseudo Inverse (NSPI) Control Allocation

The linear mapping between $\hat{u}_a$ and $\hat{u}_c$ is presented through the PI control allocation. However, the solution given by (28) may not satisfy the practical thruster range with the limitation of the thruster configuration [19]. Thus, the optimal solution can be improved by employing the null space of the control allocation matrix

$$\hat{u}_a = \hat{D}^{\mathrm{T}} \odot (\hat{D} \odot \hat{D}^{\mathrm{T}})^{-1} \odot \hat{u}_c + \hat{\zeta} \tag{29}$$

where $\hat{D} \odot \hat{\zeta} = \hat{0}$, namely $\mathrm{Null}(\hat{D}) = \{\hat{\zeta} | \hat{D} \odot \hat{\zeta} = \hat{0}\}$. Thus, the thruster output can be adjusted to the available range with the proper choice of $\hat{\zeta}$. Furthermore, $\hat{\zeta}$ can be expressed as: $\hat{\zeta} = \hat{\chi} \odot \hat{\Gamma}$, where $\hat{\chi} = [\hat{\chi}_1, \hat{\chi}_2, ..., \hat{\chi}_{n-6}]$ is the basic solution of null space, and $\hat{\Gamma} = [\hat{\Gamma}_1, \hat{\Gamma}_2, ..., \hat{\Gamma}_{n-6}]^{\mathrm{T}}$ is the undetermined coefficient. Thus, the control allocation can be described by an optimization problem

$$\begin{aligned} \min_{\hat{\zeta}_i} J &= \sum_{i=1} < \hat{\zeta}_i | \hat{\zeta}_i > = < \hat{c}_1 | \hat{\Gamma} > \\ \text{s.t.} \quad & \hat{G}_1 \odot \hat{\kappa}_1 \leq \hat{Q}_1 \end{aligned} \tag{30}$$

where $\hat{c}_1 = [\hat{\chi}_1 \odot \hat{\chi}_1, \hat{\chi}_2 \odot \hat{\chi}_2, ..., \hat{\chi}_{n-6} \odot \hat{\chi}_{n-6}]$, $\hat{G}_1 = [\hat{\chi}, -\hat{\chi}]$, $\hat{\kappa}_1 = [\hat{\Gamma}, \hat{\Gamma}]$, $\hat{Q}_1 = [\hat{u}_{am} - \hat{D}^{\mathrm{T}} \odot (\hat{D} \odot \hat{D}^{\mathrm{T}})^{-1} \odot \hat{u}_c, \hat{D}^{\mathrm{T}} \odot (\hat{D} \odot \hat{D}^{\mathrm{T}})^{-1} \odot \hat{u}_c]$, $\hat{u}_{am}$ is the maximum output capability of the actuators.

B. Simplex Method Based Improved Pseudo Inverse Control Allocation

The control allocation problem (30) can be rewritten as:

$$\begin{aligned} \min_{\hat{\zeta}_i} J &= \sum_{i=1} < \hat{\zeta}_i | \hat{\zeta}_i > = < \hat{c}_2 | \hat{\kappa}_2 > \\ \text{s.t.} \quad & \hat{G}_2 \odot \hat{\kappa}_2 = \hat{Q}_2 \end{aligned} \tag{31}$$

where $\hat{G}_2 = [\hat{G}_1, \hat{I}]$, $\hat{c}_2 = [\hat{c}_1, \hat{0}]$, $\hat{\kappa}_2 = [\hat{\kappa}_1, \hat{\kappa}_s]^{\mathrm{T}}$, $\hat{Q}_2 = [\hat{Q}_1, \hat{0}]$, and $\hat{\kappa}_s$ is the slack variable.

Theorem 2: With regard to non-singular dual sub-square matrix $\hat{G}_{2B}$, the programming problem (31) is equivalent to:

$$\begin{aligned} \min J = \; & \hat{c}_{2B} \odot \hat{G}_{2B}^{-1} \odot \hat{Q}_2 \\ & - (\hat{c}_{2B} \odot \hat{G}_{2B}^{-1} \odot \hat{G}_{2N} - \hat{c}_{2N}) \odot \hat{\kappa}_{2N} \\ \text{s.t.} \quad & \hat{\kappa}_{2B} + \hat{G}_{2B}^{-1} \odot \hat{G}_{2N} \odot \hat{\kappa}_{2N} = \hat{G}_{2B}^{-1} \odot \hat{Q}_2 \end{aligned} \tag{32}$$

where $\hat{\kappa}_{2B}$ and $\hat{\kappa}_{2N}$ are the basic variable and the non-base variable of $\hat{\kappa}_2$, respectively. $\hat{c}_{2B}$ and $\hat{c}_{2N}$ are the corresponding parts with the basic and non-base aspect of $\hat{c}_2$, respectively. $\hat{G}_{2N}$ is the sub-matrix of $\hat{G}_2$ except $\hat{G}_{2B}$.

Proof. With the block matrices defined above, the constraint condition of (31) can be written as:

$$[\hat{G}_{2B}, \hat{G}_{2N}][\hat{\kappa}_{2B}, \hat{\kappa}_{2N}]^{\mathrm{T}} = \hat{Q}_2 \tag{33}$$

where $\hat{\kappa}_{2B} = \hat{G}_{2B}^{-1} \odot (\hat{Q}_2 - \hat{G}_{2N} \odot \hat{\kappa}_{2N})$. Substituting $\hat{\kappa}_{2B}$ into (32), one can obtain

$$\begin{aligned} J &= < \hat{c}_{2B} | \hat{\kappa}_{2B} > + < \hat{c}_{2N} | \hat{\kappa}_{2N} > \\ &= < \hat{c}_{2B} | \hat{G}_{2B}^{-1} \odot (\hat{Q}_2 - \hat{G}_{2N} \odot \hat{\kappa}_{2N}) > + < \hat{c}_{2N} | \hat{\kappa}_{2N} > \\ &= < \hat{c}_{2B} | \hat{G}_{2B}^{-1} \odot \hat{Q}_2 > - < \hat{\lambda}_N | \hat{\kappa}_{2N} > \end{aligned} \tag{34}$$

where $\hat{\lambda}_N = \hat{c}_{2B} \odot \hat{G}_{2B}^{-1} \odot \hat{G}_{2N} - \hat{c}_{2N}$ is the checking number.

Remark 5: If all checking numbers of the non-base variables are less than or equal to zero, basic solution corresponding to $\hat{G}_{2B}$ will be the optimal solution of programming problem (31). If the checking number is beyond zero and the corresponding $\hat{Q}_2 \leq 0$, there exists no optimal solution of (31). If some checking numbers and the corresponding $\hat{Q}_2$ are both larger than zero, the non-base variable corresponding to the positive checking number will become the basic variable. Continuous circulation is implemented until the first condition is satisfied, and one can obtain the final optimal solution of programming problem (31).

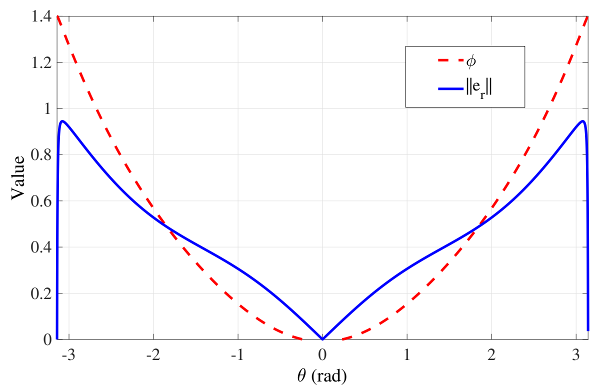

Fig. 1. Variation curve of and $\|e_r\|$ against (25)-(26).

V. Simulation Results

To verify the effectiveness of the proposed NFTSM controller (17), simulations have been carried out using the rigid spacecraft system governed by (8). A TSM controller [15] is also simulated for comparison. It is noted that the presence of the sign function in (17) will result in chattering phenomenon. To solve this problem, the hyperbolic tangent function is used as substitution of the sign function.

It is assumed that the leader spacecraft is in circular orbit with 42240 km. The control objective of the follower spacecraft is keeping the same attitude and distance with the leader. The initial relative attitude and position of the follower spacecraft are chosen as $\rho_e(0) = [-20, -10, -10]^{\mathrm{T}}$m, $q_e(0) = [0.6245, 0.5, 0.5196, 0.3]^{\mathrm{T}}$, $\rho_{ed} = [0, 0, 0]^{\mathrm{T}}$m, $q_{ed} = [1, 0, 0, 0]^{\mathrm{T}}$, $\omega_e(0) = [0, 0, 0]^{\mathrm{T}}$rad/s. The external disturbance force and torque are $u_d = [0.06 +$

$0.03\sin(0.6t), 0.05 + 0.04\sin(0.9t), 0.04 + 0.01\sin(0.5t)]^{\mathrm{T}}\mathrm{N}$ and $\tau_d = [0.00002 + 0.0005\sin(0.8t), 0.00003 + 0.0003\sin(0.5t), 0.00001 + 0.0007\sin(0.3t)]^{\mathrm{T}}\mathrm{Nm}$. The nominal mass and inertia are $m_0 = 100\mathrm{kg}$ and $J_0 = \mathrm{diag}\{18, 18, 24\}\mathrm{kgm}^2$ while the actual ones are $m = 95\mathrm{kg}$ and $J = \mathrm{diag}\{17, 17, 22\}\mathrm{kgm}^2$. The control parameters are set as: $\alpha = 0.67$, $p_1 = 0.6$, $p_2 = 0.67$, $\hat{\delta} = 0.05 + \epsilon 0.001$, $\hat{K} = \mathrm{diag}\{20, 20, 20\} + \epsilon\mathrm{diag}\{20, 20, 20\}$, $\hat{\alpha}_1 = \hat{\alpha}_2 = \hat{b} = \mathrm{diag}\{0.05, 0.05, 0.05\} + \epsilon\mathrm{diag}\{0.1, 0.1, 0.1\}$, $\hat{\alpha}_3 = \mathrm{diag}\{2, 2, 2\} + \epsilon\mathrm{diag}\{2, 2, 2\}$.

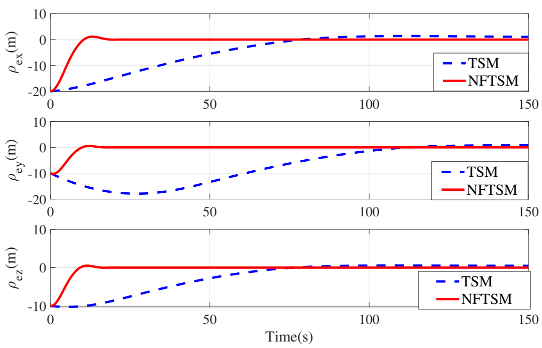

Fig. 2. Time response of ρ_e.

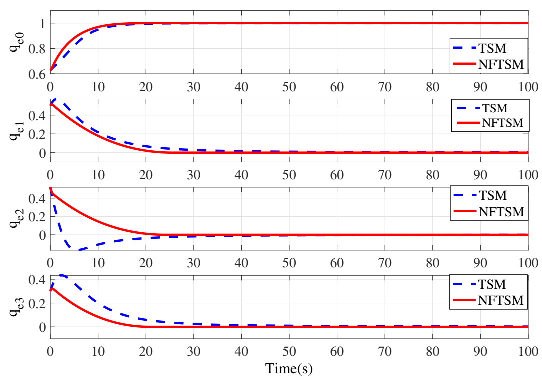

Fig. 3. Time response of q_e.

Figs. 2 and 3 represent the time responses of relative position and attitude errors, where the relative position error driven by TSM controller converges to within 78s. In contract, the proposed controller performs well because convergence rate and accuracy are both considered in the sliding mode and controller design. Thus, the relative position error driven by the proposed controller converges within 22s. In Fig. 3, the relative attitude in proposed controller converges faster than that in TSM. Note that the TSM controller leads to more transient oscillations in attitude and angular velocity responses, as shown in Figs. 3 and 4. It is noted that singularity phenomenon is eliminated in the proposed controller.

Based on the proposed controller, the following actuator configuration (see Fig. 5) is employed to test the proposed NSPI control allocation scheme using the improved simplex method. It is noted that #01-#16 denote corresponding thrusters in Fig. 5.

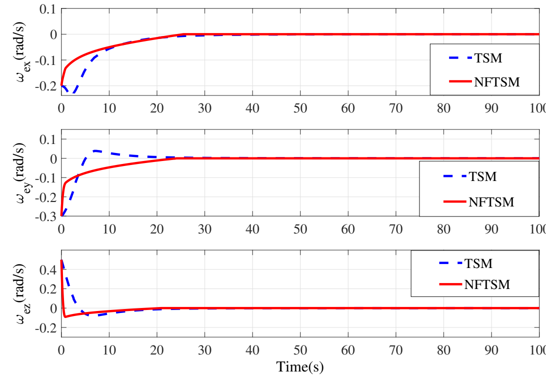

Fig. 4. Time response of ω_e.

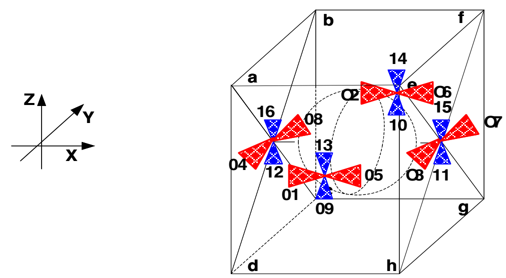

Fig. 5. Conventional thruster configuration (CTC).

Figs. 6-9 show the practical outputs of each actuator in CTC. As observed, pair-mounted actuators can provide symmetrical thrusts. The feasible solution can be found in pseudo inverse method beyond thrust limitation 5N in CTC, where the negative values can also be offered by the thruster from the other direction. Compared with the conventional PI method, the improved simplex method can achieve control allocation requirements successfully despite control force limitations.

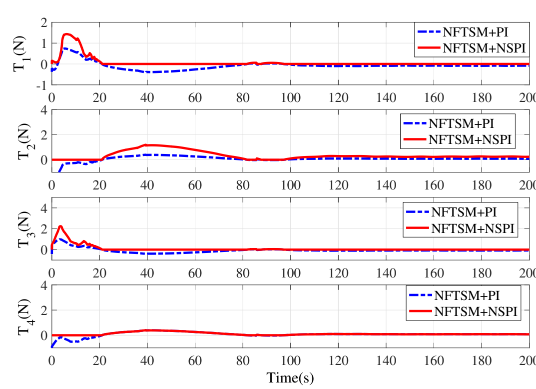

Fig. 6. Control force of thrusters #01-#04.